

## Supporting information

### Reconstructing phase of vanadium oxides enables redox-catalysis manipulated reversible sulfur conversion for stable Zn-S batteries

*Hao Luo*<sup>a,e,1\*</sup>, *Fan Li*<sup>a,b,1</sup>, *Mingli Wang*<sup>d\*</sup>, *Shang Sun*<sup>b</sup>, *Min Zhou*<sup>b</sup>, *Wenjing Zhang*<sup>b</sup>, *Hengrui Guo*<sup>a,e</sup>, *Xueyin Su*<sup>a,e</sup>, *Xiaolong Li*<sup>c\*</sup>, *Lina Ma*<sup>b\*</sup>

<sup>a</sup> School of Materials Science and Engineering, Xiamen University of Technology, Xiamen 361024, China

<sup>b</sup> College of Chemistry and Chemical Engineering, Qingdao University, Qingdao 266071, China.

<sup>c</sup> State Key Laboratory of Polymer Materials Engineering, Polymer Research Institute, Sichuan University, Chengdu 610065, P.R. China

<sup>d</sup> School of Materials Science and Engineering, Beijing University of Chemical Technology, Beijing, 100029, China

<sup>e</sup> School of Materials Science and Engineering, Zhengzhou University, Zhengzhou 450001, China

\* Corresponding author.

E-mail address: [luohao\\_hit@163.com](mailto:luohao_hit@163.com) (H. Luo)

[xiaolongli@scu.edu.cn](mailto:xiaolongli@scu.edu.cn) (X. L. Li)

[malina@qdu.edu.cn](mailto:malina@qdu.edu.cn) (L. N. Ma)

[mingliw2000@163.com](mailto:mingliw2000@163.com) (M. L. Wang)

# 1. Experimental Section

## 1.1 Materials

Vanadium(III) chloride ( $VCl_3$ , Aladdin Ltd.), terephthalic acid ( $H_2BDC$ , Aladdin Ltd.), hexadecyl trimethylammonium bromide (CTAB, National Medicine Co., Ltd.), zinc sulfate heptahydrate ( $ZnSO_4 \cdot 7H_2O$ , National Medicine Co., Ltd.), sulfur (S, National Medicine Co., Ltd.), Zinc iodide ( $ZnI_2$ , National Medicine Co., Ltd.), Poly(vinylidene fluoride) (PVDF, National Medicine Co., Ltd.), N-Methyl-2-pyrrolidone (NMP, National Medicine Co., Ltd.), carbon cloth (CC, Aladdin Ltd.). Other chemicals were purchased from Shanghai McLean Biochemical Company, and all solvents and chemicals were used as received.

## 1.2 Preparation of vanadium-based metal-organic frameworks (V-MOF)

In general, 800 mg  $VCl_3$  and 461mg  $H_2BDC$  were dissolved in an appropriate deionized solution, followed by water and vigorous agitation for 30 minutes. Then, 10mg CTAB was added into the above solution and transferred to a 50 mL Teflon-lined stainless steel autoclave, and sealed at  $200^\circ C$  for 48 h. The layered microcube V-MOF was obtained after being filtered and collected at room temperature, washed with water/ethanol three times, and dried at  $60^\circ C$  in a vacuum drying oven.

## 1.3 Preparation of $V_2O_3@C$

The V-MOF precursor was placed in a tubular furnace filled with Ar gas flow and the temperature was raised to  $700^\circ C$  at a heating rate of  $2^\circ C/min$ , after being stabilized at  $700^\circ C$  for 4h and naturally cooled to room temperature,  $V_2O_3$  wrapped in carbon matrix ( $V_2O_3@C$ ) was obtained.

## 1.3 Preparation of $V_2O_3@C/S$

The sulfur powder and  $V_2O_3@C$  were mixed in a ratio of 2:1 and ground for 20 min. Then, the mixture was sealed in a glass tube and heated to  $155^\circ C$  for 12 h, then the  $V_2O_3@C/S$  was obtained. The control sample of S/C was prepared in the same way.

## 1.4 Materials Characterization

The morphologies and microstructure of the samples were observed by a scanning electron microscope (SEM) and high-resolution transmission electron microscope (HRTEM). Elemental mapping images were collected using a SEM equipped with energy-dispersive X-ray (EDX) spectroscopy. The crystal structure of the samples was analyzed using an X-ray diffractometer

(XRD). The detailed chemical states of the elements on the surface of the composites were determined using an X-ray photoelectron spectrometer (XPS). Raman spectra were performed via the WITEC system with a laser wavelength of 532 nm. The specific surface area and textural properties were calculated by the Brunauer-Emmett-Teller (BET) and Barrett-Joyner-Halenda (BJH) methods. The thermogravimetric analysis (TGA) was carried out under the N<sub>2</sub> atmosphere to determine the sulfur content of the composite cathode.

### 1.5 Electrochemical measurements

The positive electrode was prepared by coating a slurry that was mixed with V<sub>2</sub>O<sub>3</sub>@C/S, Super-P, and PTFE at a weight ratio of 6:3:1 on a current collector, after which the mixture was dried at 50°C for 4 hours. The electrodes were cut into discs of 12 mm and the mass loading of each electrode was around 2 mg cm<sup>-2</sup>. Then, the CR-2032 type coin cell was assembled with an as-prepared positive electrode, Zn foil, Whatman filter paper, and an aqueous electrolyte composed of 3M ZnSO<sub>4</sub> solution and 75mM ZnI<sub>2</sub>. Then, the Cyclic voltammetry (CV) was tested by the CHI 660E in a voltage range of 0.1-1.5V. The electrochemical measurements were performed on a Neware BTS-4000 battery analyzer within the voltage range of 0.1-1.8 V with all capacities normalized by the weight of sulfur. Electrochemical impedance spectroscopy (EIS) measures frequencies ranging from 100 kHz to 0.01 Hz. The GITT was applied to analyze the reaction and diffusion kinetics at a current density of 100 mA g<sup>-1</sup> and a charge/discharge time and interval of 10 min for each step.

### 1.6 DFT calculation parameters

First principles density functional theory (DFT) calculations were performed using the generalized gradient approximation (GGA) with the Perdew-Burke-Ernzerhof (PBE) functional. Projected augmented wave (PAW) potentials characterized the ionic cores and included valence electrons, using a plane wave basis set with a kinetic energy cut-off of 500 eV. Gaussian smearing with a width of 0.05 eV accommodated partial occupancies of the Kohn-Sham orbitals. Electronic self-consistency was achieved when the energy variation was below 10<sup>-5</sup> eV. Geometry optimization was considered converged when the energy change was below -0.02 eV Å<sup>-1</sup>. The equilibrium lattice constants were optimized using a 3 × 2 × 1 Monkhorst-Pack k-point grid to sample the Brillouin zone. The adsorption energies ( $\Delta E_a$ ) were calculated as  $\Delta E_a = E_{a/sub} - E_{sub} - E_a$ , where  $E_{a/sub}$ ,  $E_{sub}$ , and  $E_a$  are the total energies of the optimized adsorbate/substrate system, the bare substrate, and the adsorbate in the structure,

respectively. The free energy ( $\Delta G$ ) calculations of each elementary step were based on the standard hydrogen electrode model, which can be determined as:  $\Delta G = \Delta E + \Delta \text{EZPE} - T\Delta S - neU$ , where  $\Delta E$  and  $\Delta S$  are the reaction energy and entropy change;  $\Delta \text{EZPE}$  is the difference in zero-point energy between the adsorbed and the gas phase molecules;  $U$  is the applied bias and  $n$  is the electron transfer number involved in the reaction. Here  $U = 0 \text{ V}$  for free energies diagrams demonstrated in the paper.

## 2. Supplementary Figures



**Figure S1.** SEM images of V-MOF.

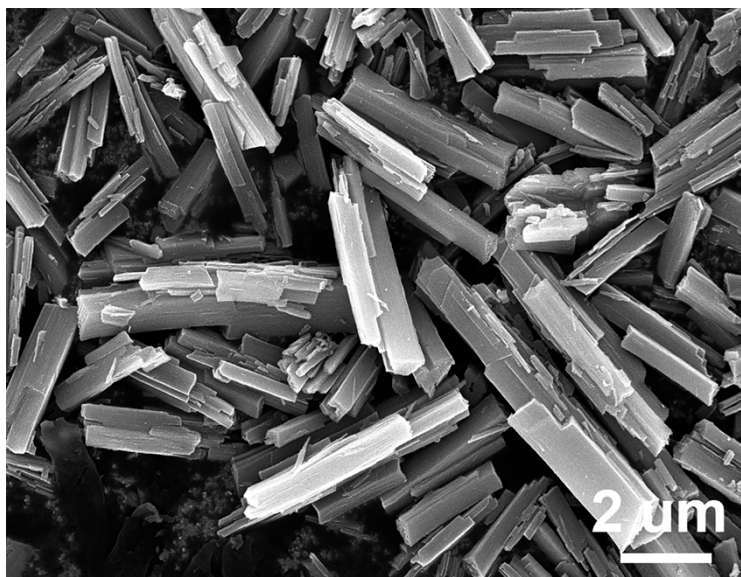


**Figure S2.** SEM images of V<sub>2</sub>O<sub>3</sub>@C.

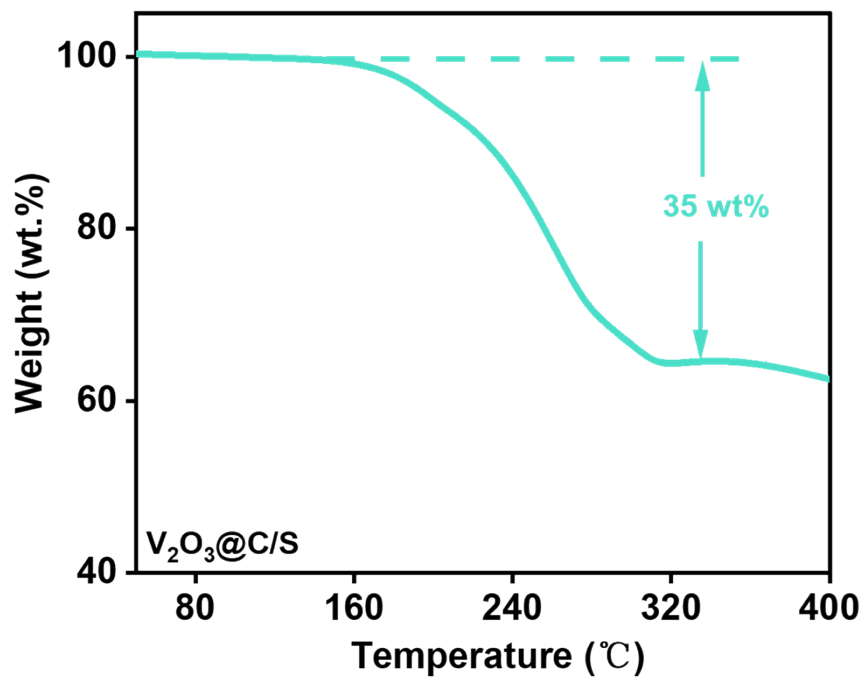


Figure S3. Thermogravimetric curve of  $V_2O_3@C/S$ .

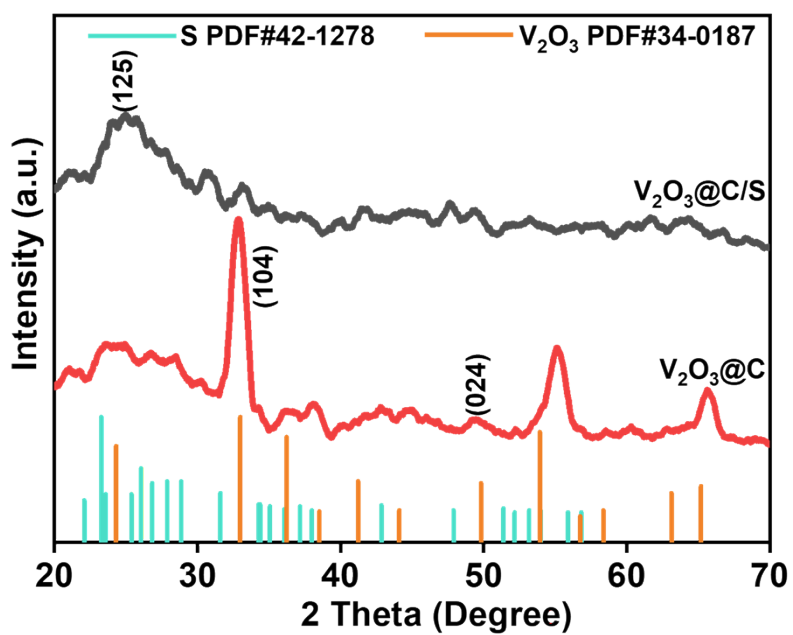


Figure S4. The XRD spectrum of  $V_2O_3@C$  and  $V_2O_3@C/S$ .

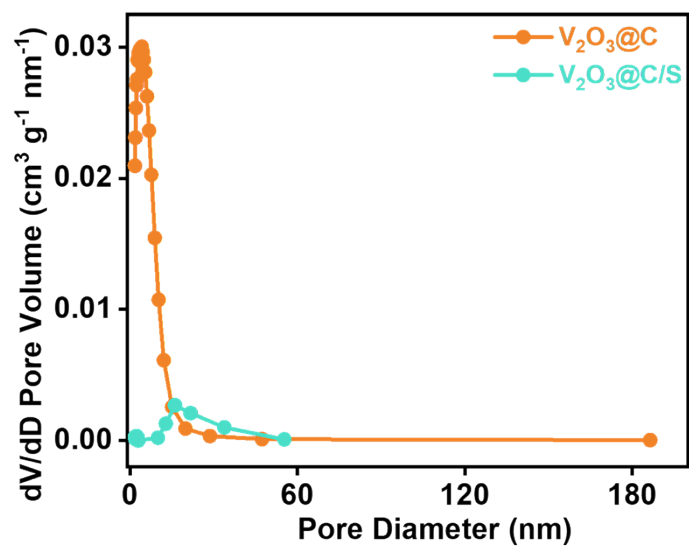


Figure S5. Pore-size distribution curves of different samples.

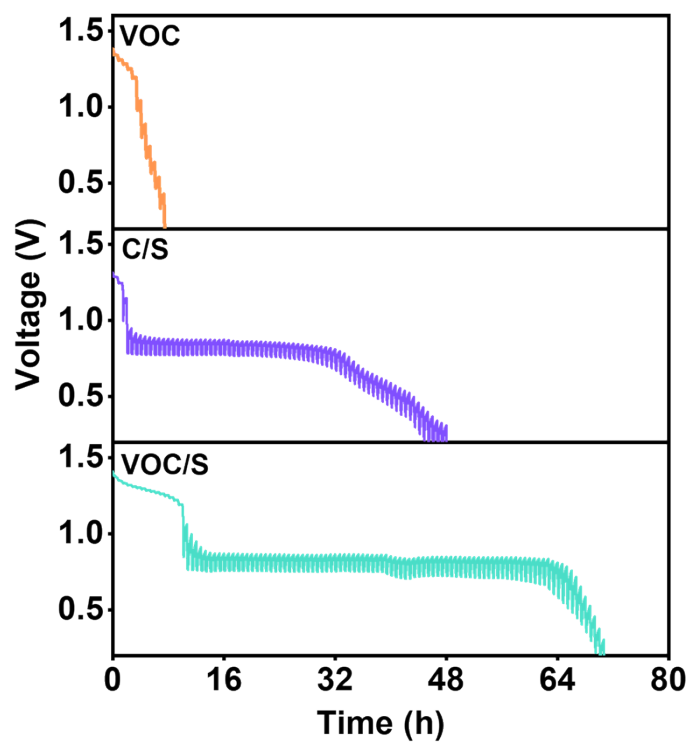
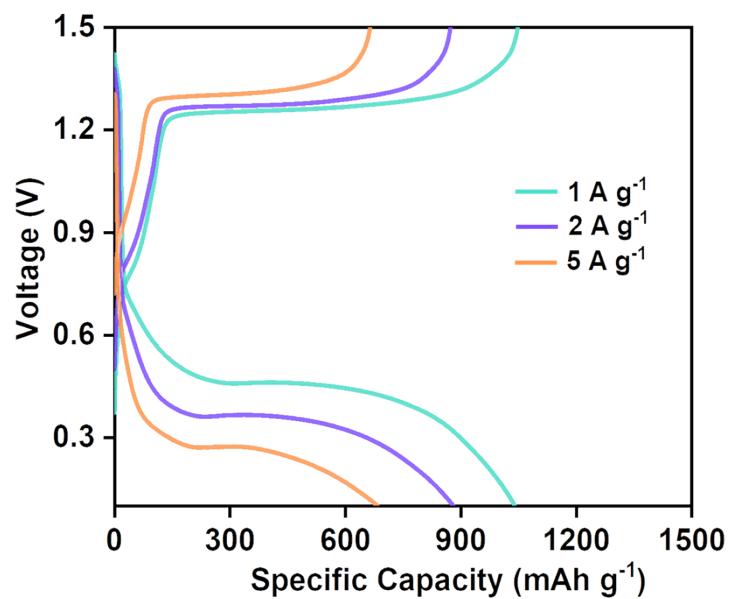
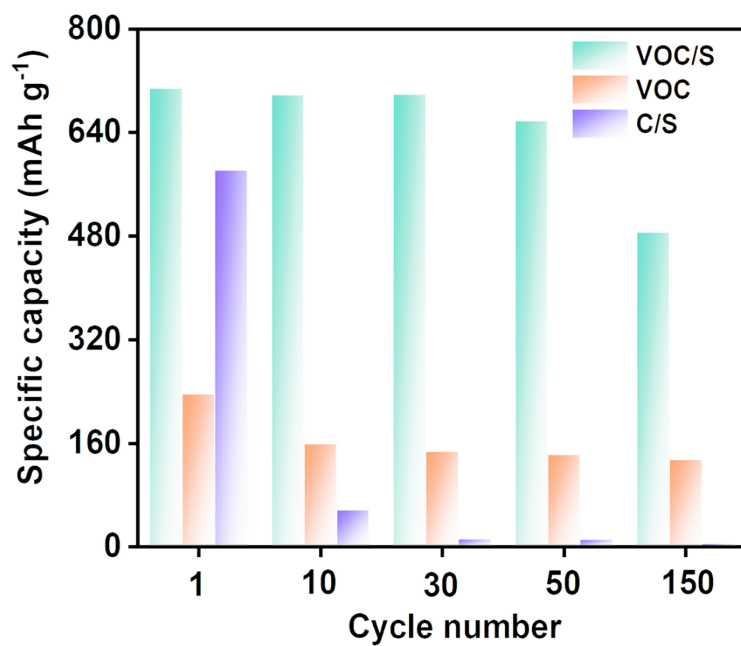


Figure S6. The GITT curves of VOC, C/S, and VOC/S at 100 mA g<sup>-1</sup>.



**Figure S7.** GCD curves at different current densities of VOC/S.



**Figure S8.** Cycle number and specific discharge capacity at 4 A g<sup>-1</sup> of VOC/S.



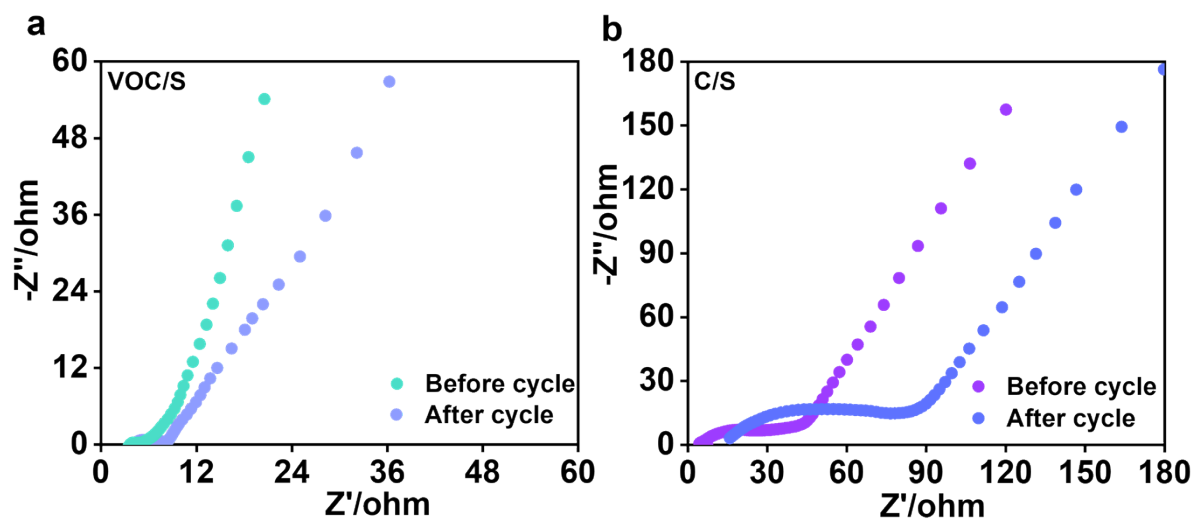


**Figure S9.** EIS curves of (a) VOC/S and (b) C/S cathodes were recorded before and after the cycling test.

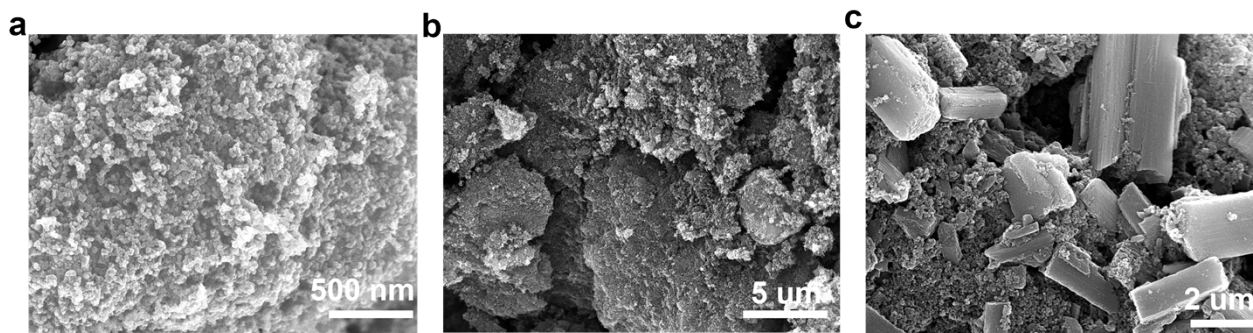


**Figure S10.** (a) SEM images of the fresh C/S cathode; SEM images of the (b) C/S and (c) VOC/S cathode after the 150 cycles at  $4 \text{ A g}^{-1}$ .

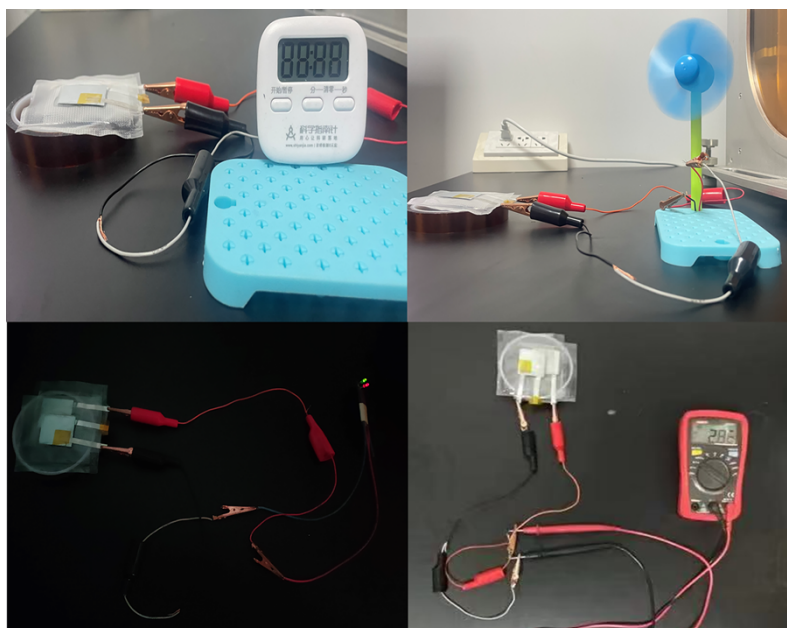


**Figure S11.** Performance of flexible Zn-S pouch cells.

### 3. Supplementary Tables

**Table S1.** Pore size distribution of the sample.

Sample	Adsorption average pore diameter	BJH Desorption average pore diameter
V <sub>2</sub> O <sub>3</sub> @C	5.4080 nm	4.5784 nm
V <sub>2</sub> O <sub>3</sub> @C/S	31.9637 nm	27.0837 nm